

## CFD-based design algorithm for CO2 ejectors

Knut RINGSTAD<sup>(a)</sup>, Krzysztof BANASIAK<sup>(b)</sup>, Armin HAFNER<sup>(a)</sup>

<sup>(a)</sup> Norwegian University of Science and Technology,  
Kolbjørn Hejes vei 1B, 7491 Trondheim, Norway

<sup>(b)</sup> SINTEF Energy, Kolbjørn Hejes vei 1d, 7465 Trondheim, Norway  
[knut.e.ringstad@ntnu.no](mailto:knut.e.ringstad@ntnu.no)

### ABSTRACT

In this work, a novel CFD-database generation algorithm for CO2 ejectors are presented. The algorithm is explained and its details discussed. A case for CFD database generation is then performed based on an ejector design for an industry client. The ejector design is investigated with different design parameters around the suggested design. Design improvements are suggested based on the numerical results, and a final design is suggested. The final design had a high ejector efficiency of simulated to be 46% at the design point, and the ejector performance is evaluated and discussed for off-design conditions.

Keywords: R744, Ejector, Computational Fluid Dynamics, Numerical Modelling, Ejector design

### 1. INTRODUCTION

The transition to more environmentally friendly solutions is accelerating. In the HVAC industry, a lot of research has been focused on natural and environmentally friendly working fluids. Of the natural refrigerants, CO2 systems is considered to be a highly efficient and cost-effective solution for many applications.

CO2 systems can in many situations be significantly improved by the introduction of ejector solutions. Ejectors are work-recovery devices that by utilizing the expansion of a high pressure ‘motive’ to pump a secondary ‘suction’ flow from a low pressure. The ratio of entrained suction flow to motive flow is referred to as the entrainment ratio (ER), see Eq. (1):

$$ER = \frac{\dot{m}_s}{\dot{m}_m} \quad \text{Eq. (1)}$$

The efficiency of the ejector can then be defined by ratio of actual to maximum theoretical recovered work, defined in Eq. (2), described in detail by Elbel and Lawrence (2016):

$$\eta_{ejector} = ER \frac{h_{s,iso} - h_s}{h_m - h_{m,iso}} \quad \text{Eq. (2)}$$

Increasing use of ejector solutions has encouraged more research into ejector design and modelling. In recent years, emphasis has been put on the development of advanced CFD models for the prediction of CO2 ejector performance (Giacomelli et al. 2019, Bodys et al. 2020, He et al. 2019). For a detailed review of CO2 ejector model development, see Ringstad et al. 2020.

CFD based algorithms for ejector design have been presented in previous works (Palacz et al 2016, Palacz et al 2017). Palacz et al. (2016-2017) presented a shape optimization algorithm based on the EjectorPL algorithm. In these works, a genetic optimization algorithm was used to look for design improvements for 6 geometry shape parameters, namely; mixing chamber diameter, mixing chamber length, motive nozzle, premixing chamber length, motive nozzle converging and diverging angle, and motive nozzle outlet diameter. Recently, He et al. (2021) investigated the covariation between 3 geometric shape parameters and the exergy production of the flow. Their study found that the synergetic effects of several ejector parameters must be considered simultaneously to identify design improvements. Similar findings were reported by Banasiak et al. (2014).

In this work, the homogeneous equilibrium two-phase ejector CFD model is implemented into a fully automated algorithm for generation of CFD databases. The CFD database is then used to design an ejector for an industry client for application in a new heat-pump system. The design is investigated for off-design conditions.

## 2. MULTIPHASE MODEL

In this work, a homogeneous equilibrium model (HEM) is used for calculation of two-phase flow of CO<sub>2</sub> in the ejector. The model is implemented in ANSYS v.19.3 with user-defined-functions for fluid properties and enthalpy transport.

The HEM is based on an enthalpy-formulation implemented developed by Smolka et al. (2013). The model assumes thermodynamic, thermal and mechanical equilibrium between the phases. The averaged set of equations for the liquid and vapor phase are then presented as, Eq. 1-3:

$$\frac{\partial \rho_m}{\partial t} + \frac{\partial}{\partial x_j} [\rho_m u_{mj}] = 0, \quad \text{Eq. (3)}$$

$$\frac{\partial}{\partial t} (\rho_m u_{mi}) + \frac{\partial}{\partial x_j} [\rho u_{mi} u_{mj} + p_m \delta_{ij} - \tau_{mij}] = 0, \quad \text{Eq. (4)}$$

$$\nabla \cdot (\rho \vec{u} h) = \nabla \cdot (k_{\text{eff}} \nabla h) + \dot{S}_{h1} + \dot{S}_{h2} + \dot{S}_{h3}, \quad \text{Eq. (5)}$$

Here,  $h$  is the specific enthalpy,  $\vec{u}$  is the velocity vector,  $k_{\text{eff}}$  the effective diffusion coefficient, and the source terms  $\dot{S}_{h1,2,3}$  describe the mechanical energy, the irreversible dissipation of the kinetic energy variations and the dissipation of the turbulent kinetic energy, respectively (Smolka et al., 2013). The thermodynamic state is then uniquely defined at homogeneous equilibrium by the pressure and enthalpy:

At homogeneous equilibrium, the enthalpy and pressure uniquely define a thermodynamic state in the two-phase dome (Eq. 6):

$$\rho, \mu, k, \alpha, T, q, c = f(p, h) \quad \text{Eq. (6)}$$

In addition, the k-epsilon Realizable turbulence model with scalable wall functions is used as the turbulence model.

## 3. DATABASE GENERATION TOOL

### 3.1. Database layout

The database is organized in cases for ease of use. A case contains a collection of results, meshes, post-processing and algorithm settings. The settings can be changed for each ejector design to user specifications, such as changing CFD settings, meshing settings, and sampling algorithm settings.

#### 3.1.1. Parameters and database sampling

Each case will contain a separate database of model parameters. The model parameters are changeable and more parameters can be added depending on case requirements. The parameters contain the CFD model parameter, boundary condition and shape parameters that decide the ejector design and operating condition. The database also contains several outputs, such as predicted mass flow rates and other performance indicators.

Each parameter can be defined as a feature; a feature is a parameter that is sampled in the database. The remaining parameters are kept at the predefined baseline conditions. The sampling can be done via linear sampling between two values, which can use a space filling or a latin hypercube design to sample the feature-space. For the ejector design algorithm, a list of 16 geometry parameters and 5 boundary condition values are used for a calculation. In this work, the studied features will be motive nozzle throat diameter,  $D_t$ , the motive nozzle outlet diameter,  $D_{mo}$ , and the mixing chamber length,  $L_{mix}$  and diameter,  $D_{mix}$ .

#### 3.1.2. Properties

For these calculations a look-up table for CO<sub>2</sub> is used in the HEM model generated using the CoolPack library. However, the algorithm can easily be interchanged with other working fluids.

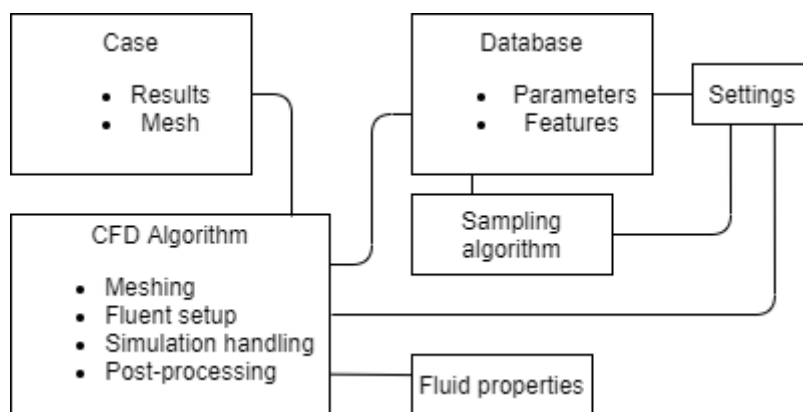


**Figure 1: Database layout**

### 3.2. Numerical solver and setup

The numerical solver is a Pressure-based Coupled solver for 2D axisymmetric flow. The second order upwind discretization schemes are used for momentum,  $k$ , epsilon, and enthalpy transport variables and the PRESTO scheme for pressure. A steady solver was used with a CFL number that was stepped up from 0.3 to 0.5 during simulation.

Inlets are defined as pressure inlets with constant value Dirichlet boundary conditions. The ejector outlet is defined as a pressure outlet, with a Neumann zero gradient boundary condition for enthalpy. A turbulence intensity of 5% and a turbulent viscosity ratio of 10 was specified at all inlets and outlets. A wall roughness of 2 micrometers, adiabatic and no-slip boundary conditions are applied to the ejector walls. The pressure and enthalpy boundary conditions at motive inlet, suction inlet and outlet were defined based on inputs from the database.

### 3.3. Grid generation algorithm

The meshes were generated using ANSYS ICEM with an automated script for geometry setup using RPL files. The script uses the 16 inputs from the database to generate the geometry. The geometry is then meshed automatically based on the specified meshing settings. The generated meshes are of high orthogonal quality and refined in regions of large flow variation. The script is capable of 2D and 3D meshes, however due to computational load the 2D meshes are used in this work. Several numerical mesh study have been conducted for similar ejectors using the HEM model (Smolka et al. 2013). In general, these works have found that approximately 20-40k cells is adequate to reproduce ejector flow. Different meshes were also tested in this work and negligible difference was found between the X cell mesh and Y cell mesh.

### 3.4. Convergence

The computations were done on a 2xAMD Epyc 24-core processor computer with 2.0 GHz clock speed. On 8 parallel cores the computations took approximately 2-4 hours to reach the specified convergence criterion for the 70k cell mesh. The script is also capable of running on a remote cluster for computational speed up, however this capability was not used in this work.

### 3.5. Graphical User Interface

To simplify ejector design experience a graphical user interface (GUI) was implemented. The GUI allows the user to select the parameter starting values and see how the selection affects the ejector geometry design. This allows for better understanding and speed in the ejector design process.

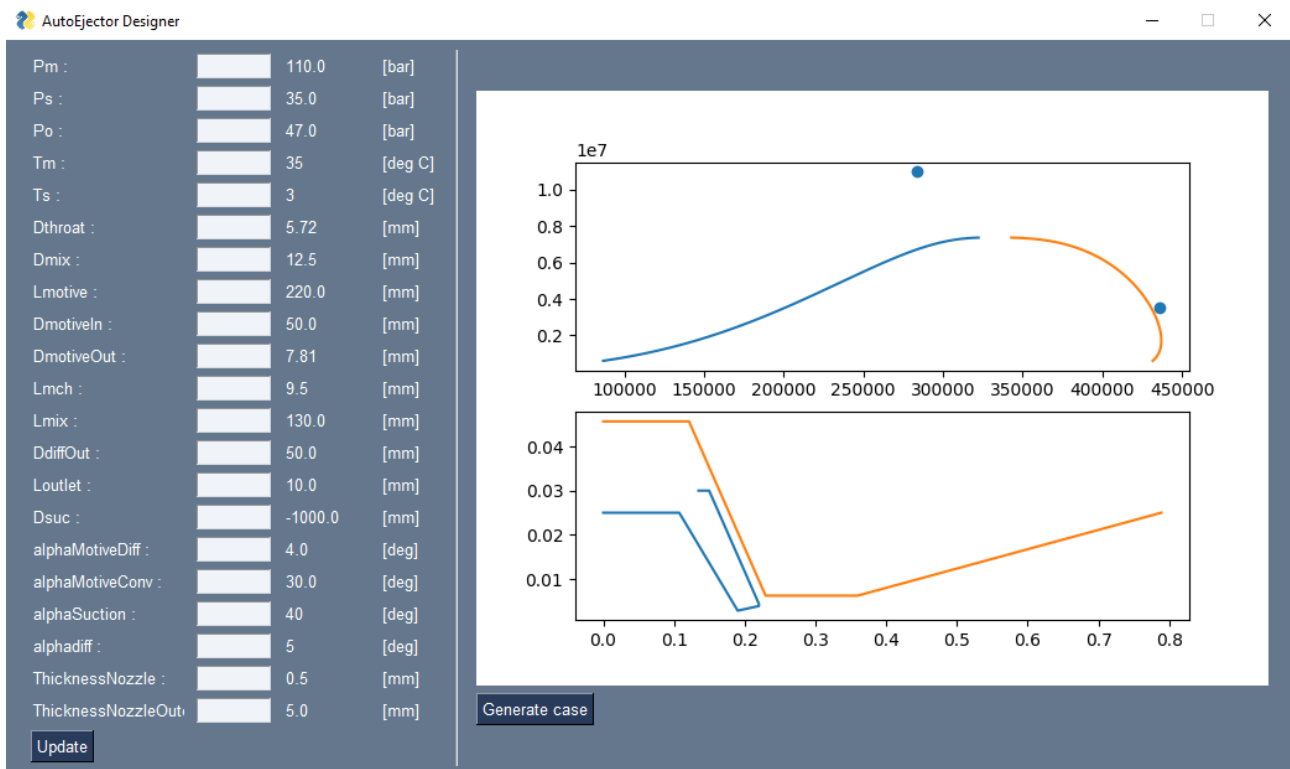


**Figure 2: Graphical user interface**

### 3.6. Autoejector design methodology

The database algorithm AutoEjector is employed for rapid CFD based ejector design. The design case is an ejector for heat pump applications that will be scaled up from a smaller design. The design process is done in three stages:

- (i) Motive nozzle design matching at design point
- (ii) Mixing chamber optimization
- (iii) Off-design performance mapping

The initial step is required to tune the mass flow rate of the ejector. The ejector motive nozzle throat diameter is increased until the specified mass flow rate is reached. Using a set motive nozzle converging and diverging angle, the motive nozzle geometry is then defined by the motive outlet diameter,  $D_{mo}$ . The motive outlet diameter is then increased until pressure matching with the mixing chamber pressure.

The second step is to design an efficient mixing chamber. The mixing chamber diameter and length are investigated with a large database of varied mixing lengths and diameters. The optimal design is then judged based on these results. Other parameters were not judged in this methodology. However, the eventual goal is to combine this tool with machine learning to optimize entire ejector geometry in this step.

The last step is to evaluate the ejector at off design conditions. This is done by sampling the ejector performance at different pressure lifts and motive pressure conditions. Also this step is planned to be automated with a machine learning algorithm for performance mapping.

## 4. RESULTS AND DISCUSSION

### 4.1. Design investigation

The design specifications by the industry client was an ejector with motive mass flow rate of 2.5 kg/s at the design point: motive pressure 110 bar, motive temperature 37° C, suction pressure 35 bar, suction temperature 5°C superheat, pressure lift 12 bar.

The design investigation was carried out according to the predefined design methodology. This was done by generating one database for each design stage, i.e. one for motive throat and outlet diameter, one for mixing section diameter and length, and one for varied pressure lift.

**Table 1. Motive nozzle throat diameter design**

<i>Design parameter</i>	<i>Value [mm]</i>	<i>Motive MFR [kg/s]</i>
Dthroat	5.72	1.53
	6	1.69
	6.5	1.98
	7	2.29
	7.5	2.64
	7.12	2.37
	7.24	2.45
	7.36	2.54

Table 2 shows the predicted motive mass flow rates with varied motive nozzle throat diameter. As the HEM will in cases under predict the motive mass flow rate, the design value was set to 7.3 mm, giving a motive mass flow rate of 2.48 kg/s.

The motive nozzle outlet diameter is the parameter that decides the motive nozzle flow expansion and must be tuned for the design point flow. The results are shown in Table 3. An outlet diameter of D<sub>mo</sub>=9.7 mm was chosen and the expansion profile was verified to be close to ideal for the design point.

**Table 2. Motive nozzle outlet diameter design**

<i>Design parameter</i>	<i>Value [mm]</i>	Jet flow
D <sub>mo</sub>	9.0	Under expanded
	9.2	Under expanded
	9.5	Slightly underexpanded
	10.5	Slightly over expanded
	12.0	Severly over expanded
	13.0	Severly over expanded

In the second design stage, the mixing chamber will be optimized to maximize suction flow. For proprietary reasons the full ejector geometry will be presented in non-dimensional form, as a ratio between the design parameter and the final design parameter. The mixing chamber diameter was calculated based on the ratio of D<sub>mix</sub>/D<sub>throat</sub> and neighbouring datapoints were sampled. The results are shown in Table 3.

**Table 3. Mixing chamber diameter design,  $L/L_{final} = 0.76$** 

<i>Design</i>	<i>D<sub>mix</sub> / D<sub>mix_final</sub></i>	<i>Suction MFR [kg/s]</i>
I	0.91	0.91
II	0.94	1.01
III	0.97	1.11
IV	1	1.17
V	1.06	1.14
VI	1.17	0.81

Based on these results the mixing diameters with the highest suction mass flow rate (III, IV, V) were further tested by co-variation of  $L_{mix}$  and  $D_{mix}$ . The results are shown in Table 4. The mixing length had a minor effect on suction mass flow rate. The final design was chosen based on the best performance of the resulting geometries.

**Table 4. Mixing chamber length and diameter design**

<i>D<sub>mix</sub> / D<sub>mix_final</sub></i>	<i>L<sub>mix</sub> / L<sub>mix_final</sub></i>	<i>Suction MFR [kg/s]</i>
0.97	1	0.993
0.97	1.06	1.013
0.97	1.17	1.010
1	1	1.195
1	1.06	1.191
1	1.17	1.186
1	1.2	1.171
1.06	1	1.184
1.06	1.06	1.177
1.06	1.17	1.166
1.06	1.27	1.097

With the optimized design at design point the ejector efficiency was calculated to be 46%.

#### 4.2. Off-design performance

Lastly, the ejector performance is tested at different pressure lifts, shown in Table 5. The results indicate that the ejector design is able to operate at pressure lifts up to 17-18 bar. The maximum efficiency of the ejector is at the design point of 12 bar, and the efficiency quickly drops off beyond 14 bar of pressure lift.

**Table 5. Off- design performance at varied pressure lifts**

Pressure lift (bar)	Motive mass flow rate kg/s	Suction mass flow rate kg/s	Ejector efficiency (-) Eqn. (2)
8	2.482	1.260	0.30
10	2.482	1.258	0.39
12	2.482	1.195	0.46
14	2.482	0.898	0.42
16	2.482	0.403	0.22
18	2.482	-0.084	-0.05

Figure 3 shows the velocity in the mixing chamber distribution for the different pressure lifts. The flow clearly transitions from a long shock train to a short core with high velocity flow as the pressure lift increases. It also illustrates the suction flow going from super-sonic choked flow to sub-sonic flow for higher pressure lifts.

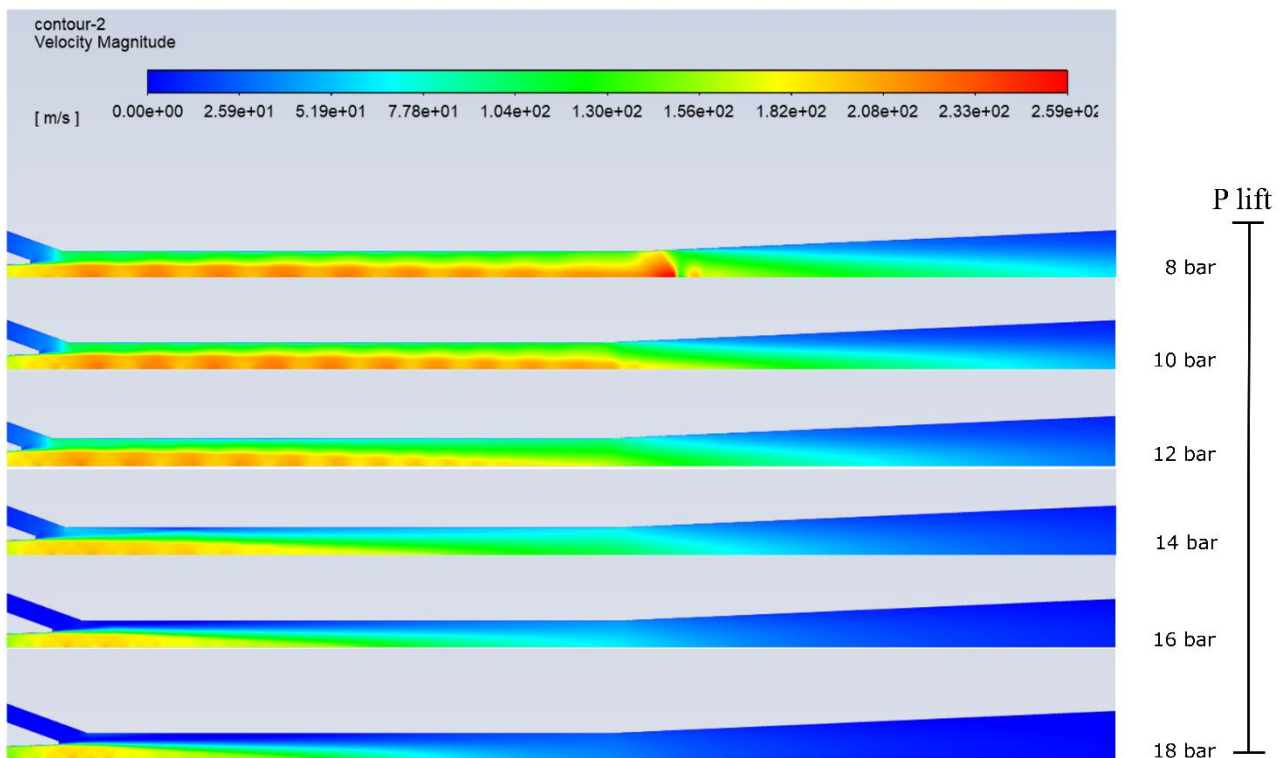


**Figure 3: Velocity distribution in mixer and diffuser at different pressure lifts**

The full 2D or 3D flow distribution, as shown in Figure 3, gives an exceptional tool for flow investigation that is not available for simpler 0D or 1D approaches. As an example, these models are able to identify flow vortices that hinder suction flow, or in detail describe the mixing process in various parts of the ejector. Since CFD modelling is based on fewer assumptions than alternative 0D or 1D approaches, it can also be applied to a wider range of geometries and flows, that are outside the scope of the simpler approaches. The cost of using CFD in comparison to other approaches is the computational cost, as calculating a single operating point can take hours in comparison to minutes with lower dimensional approaches.

### 4.3. Discussion

The CFD-based database design algorithm shows great promise for rapid testing of different geometries and operating conditions. Automatic meshing and CFD setup reduced design time dramatically and reduces the probability of setup or meshing errors. The design methodology presented shows that this approach can identify efficient ejector designs, and is an ideal candidate of automation. A fully automated design algorithm based on this approach is left for further work.

Another potential application for this database design tool is to generate data samples for a machine learning algorithm. This work is under way, and could potentially identify more optimal designs by using advanced optimization methods on ejector design data.

## 5. CONCLUSIONS

An automated approach for generation of CFD databases of ejectors is presented. This approach can generate CFD data for a generic ejector geometries and at a wide range of operating conditions. The layout and structure of the program is explained and discussed and the algorithm is used for an ejector design case for an industry partner. The algorithm was able to drastically speed up the design process and gave an efficient final design.

The benefits of using CFD models is discussed and the ejector operation at off-design pressure lifts are investigated.

## ACKNOWLEDGEMENTS

The work is part of HighEFF - Centre for an Energy Efficient and Competitive Industry for the Future, an 8-year Research Centre under the FME-scheme (Centre for Environment-friendly Energy Research, 257632/E20). The authors gratefully acknowledge the financial support from the Research Council of Norway and user partners of HighEFF.

## NOMENCLATURE

*CFD* Computational fluid dynamics                      *ER*      Entrainment ratio  
*HEM* Homogeneous Equilibrium Model

## REFERENCES

- Banasiak, K., Hafner, A., 2011. 1D Computational model of a two-phase R744 ejector for expansion work recovery. *International Journal of Thermal Sciences*, 50(11), 2235-2247.
- Banasiak, K., Palacz, M., Hafner, A., Buliński, Z., Smółka, J., Nowak, A. J., Fic, A., 2014, A CFD-based investigation of the energy performance of two-phase R744 ejectors to recover the expansion work in refrigeration systems: An irreversibility analysis, *International Journal of Refrigeration* 40, 328–337. URL:<https://www.sciencedirect.com/science/article/pii/S0140700713003812>. DOI: 10.1016/j.ijrefrig.2013.12.002.
- Elbel, S., Lawrence, N., 2016, Review of recent developments in advanced ejector technology, *International Journal of Refrigeration*, 62, pp. 1-18, 10.1016/j.ijrefrig.2015.10.031 URL: <https://www.sciencedirect.com/science/article/pii/S0140700715003266>
- He, Y., Deng, J., Li, Y., Zhang, X., 2021. Synergistic effect of geometric parameters on CO2 ejector based on local exergy destruction analysis, *Applied Thermal Engineering*, Volume 184, 116256, ISSN 1359-4311, DOI: <https://doi.org/10.1016/j.applthermaleng.2020.116256>.
- He, Y., Deng, J., Li, Y., Ma, L., 2019, A numerical contrast on the adjustable and fixed transcritical CO2 ejector using exergy flux distribution analysis, *Energy Conversion and Management*, Volume 196, Pages 729-738, ISSN 0196-8904, <https://doi.org/10.1016/j.enconman.2019.06.031>.
- Palacz, M., Smolka, J., Kus, W., Fic, A., Bulinski, Z., Nowak, A. J., Banasiak, K., Hafner, A., 2016, CFD-based shape optimisation of a CO2 two-phase ejector mixing section, *Applied Thermal Engineering* 95 62–69. URL: <https://www.sciencedirect.com/science/article/pii/S1359431115012478>. DOI: 10.1016/j.applthermaleng.2015.11.012.
- Palacz, M., Smolka, J., Nowak, A. J., Banasiak, K., Hafner, A., 2017, Shape optimisation of a two-phase ejector for CO2 refrigeration systems, *International Journal of Refrigeration* 74 210–221. URL: <https://www.sciencedirect.com/science/article/pii/S0140700716303425>. DOI: 10.1016/j.ijrefrig.2016.10.013.
- Ringstad, K. E. Allouche, Y., Gullo, P., Ervik, Å., Banasiak, K., Hafner, A., A detailed review on CO2 two-phase ejector flow modeling, *Thermal Science and Engineering Progress*, Volume 20, 2020, 100647, ISSN 2451-9049, <https://doi.org/10.1016/j.tsep.2020.100647>.
- Smolka, J., Bulinski, Z., Fic, A., Nowak, A. J., Banasiak, K., Hafner, A., A computational model of a transcritical R744 ejector based on a homogeneous real fluid approach, *Applied Mathematical Modelling* 37 (2013) 1208–1224. DOI: 10.1016/j.apm.2012.03.044.